arXiv:cond-mat/0004265v1 [cond-mat.str-el] 17 Apr 2000

Ferromagnetism and phase separation in one-dimensional d–p and periodic Anderson models

M. Guerrero
Theoretical Division, Los Alamos National Laboratory, Los Alamos, NM 87545

R.M. Noack
Institut de Physique Théorique, Université de Fribourg, CH–1700 Fribourg, Switzerland

(April 14, 2000)

Using the Density Matrix Renormalization Group, we study metallic ferromagnetism in a one–dimensional copper–oxide model which contains one oxygen p–orbital and one copper d–orbital. The parameters for the d–p model can be chosen so that it is similar to the one–dimensional periodic Anderson model. For these parameters, we compare the ground–state phase diagram with that of the Anderson model and find a ferromagnetic region analogous to one found in the Anderson model, but which is pushed to somewhat higher densities and interaction strengths. In both models, we find a region within the ferromagnetic phase in which phase separation between a localized ferromagnetic domain and a weakly antiferromagnetic regime occurs. We then choose a set of parameter values appropriate for copper–oxide materials and explore the ground–state phase diagram as a function of the oxygen–oxygen hopping strength and the electron density. We find three disconnected regions of metallic ferromagnetism and give physical pictures of the three different mechanisms for ferromagnetism in these phases.

I. INTRODUCTION

The nature of the microscopic description of metallic ferromagnetism, as found in transition metals such as iron, nickel and cobalt, is a long-standing problem in strongly correlated electron systems. The Hubbard model was formulated in the 1960's[1] in order to describe ferromagnetism in such materials. However, a ferromagnetic ground state in the single–band Hubbard model on nonfrustrated bipartite lattices has not been found at physical parameter values, and can be excluded in a large portion of the ground–state phase diagram. While mean–field theory yields a large region of stable ferromagnetism, fluctuations tend to destabilize the ferromagnetic phase, and numerical and variational calculations have narrowed the possible extent of a ferromagnetic state to a small region around the Nagoaka point. Therefore, it has become clear that additional features must be added to provide a description of metallic ferromagnetism.[2,3]

Recently, a number of such possible extensions to the Hubbard model have been investigated. In particular, there are three classes of additions which can enhance ferromagnetism: *(i)* a change in the noninteracting density of states through the addition of frustrating hopping terms or the treatment of a geometrically frustrated lattice *(ii)* the inclusion of multiple orbitals per site or unit cell, and *(iii)* the addition of more general nearest–neighbor interactions.[2,3] In relation to *(i)*, Vollhardt et al.[3] have emphasized that peaks or singularities in the occupied portion of the noninteracting density of states minimizes the kinetic energy loss due to polarization of the electrons. This picture is supported by numerical calculations in one[4] and two dimensions,[5] and within the Dynamical Mean-Field Theory with a number of different forms of the noninteracting density of states.[3] In addition, Mielke[6] has shown rigorously that a Hubbard model with a less than half–filled flat band has a fully polarized ground state. This theorem has been extended to the case of nearly flat bands.[7] For *(ii)*, a number of multiband models, such as the periodic Anderson model, the Kondo lattice model, and the multiband Hubbard models with Hund's rule coupling have been found to have ferromagnetic ground states.[2] In relation to *(iii)*, Strack and Vollhardt[8] have studied a quite general form of the nearest–neighbor interaction and have found a fully polarized ground state at half–filling and one hole from half–filling (the Nagaoka state) under certain conditions.

In this paper, we consider a one–dimensional model which contains elements of points *(i)* and *(ii)* from above. The model which we will study is a Cu–O chain that contains one oxygen p–orbital and and copper d–orbital. Since one–dimensional models can usually be treated using well-controlled analytical or numerical techniques, one can obtain a complete picture of the ground–state phase diagram without resorting to approximations necessary in two or three dimensions. For one–dimensional systems with nearest–neighbor hopping and an arbitrary, but real and particle–symmetric interaction, a theorem by Lieb and Mattis[9] rules out a magnetized ground state. Because the Lieb–Mattis theorem no longer applies when electrons can pass around each other, the minimal addition to the one–dimensional Hubbard model necessary to obtain ferromagnetism is a next–nearest–neighbor hopping. The resulting Hubbard model on a "zigzag" ladder has a ferromagnetic ground state in a substantial parame-

ter regime.[4] One can also formulate more general, related models composed of triangular elements. Two such models, studied by Tasaki[10] and Penc et al.[11] have been found to have ferromagnetic phases. The d–p model we study here is (aside from an added near–neighbor Coulomb repulsion) a particular case of the model studied in Ref. 11.

Another approach to ferromagnetism in one–dimensional models, involving point *(ii)* from above, are models with multiple non-degenerate orbitals per site. The simplest of these models are the one–dimensional Periodic Anderson Model (PAM) and the Kondo Lattice model (KLM). Both of these models have ferromagnetic ground states in a relatively large parameter regime.[12,13] These models can be related to one another in the regime of large f–repulsion for the PAM and small Kondo coupling for the KLM. The PAM is similar to the d–p model in that there are two linked non-degenerate levels per unit cell, and, as we will discuss in more detail in the following, exhibit similar behavior with the appropriate choice of parameters.

Another motivation for studying the d–p model is the relationship with models for the CuO_2 planes of the high–T_c superconductors. One dimensional d–p models have been thought to contain some of the essential ingredients needed to describe superconductivity in CuO_2 planes.[14] Because of this, previous work on the one–dimensional d–p model has concentrated on determining the conditions under which superconducting correlations are dominant for models with[15] and without[16–18] direct hopping between the p–orbitals.

In this work, we will concentrate on the ferromagnetic phases in the ground state phase diagram and will discuss their physical origin. In Sec. II, we introduce the models which we will study and discuss choices of the models parameters. In Sec. III A, we compare the phase diagram of the Anderson lattice model from Ref. 12 with that of the d–p model. We find that the ferromagnetic region persists in the d–p model but it is pushed to higher values of the interaction and higher fillings. There is a region of phase separation in which ferromagnetic and antiferromagnetic states coexist. In Sec. III B, we set the parameters of the d–p system to realistic values for the cuprates. We then investigate the phase diagram as a function of the oxygen–oxygen hopping amplitude, t_{pp}, and the band filling, and find three disconnected ferromagnetic regions with three physically different mechanisms.

II. MODELS

We consider a one-dimension d–p system with Hamiltonian

$$\begin{aligned} H = & -t_{pp}\sum_{[jj']\sigma}(p^\dagger_{j\sigma}p_{j'\sigma}+p^\dagger_{j'\sigma}p_{j\sigma})+\Delta\sum_{j\sigma}n^p_{j\sigma}+U_p\sum_j n^p_{j\uparrow}n^p_{j\downarrow} \\ & + \ U_d\sum_i n^d_{i\uparrow}n^d_{i\downarrow}-t_{pd}\sum_{<ij>\sigma}(d^\dagger_{i\sigma}p_{j\sigma}+p^\dagger_{i\sigma}d_{j\sigma})+V_{pd}\sum_{<ij>}n^d_i n^p_j\ , \end{aligned} \tag{1}$$

where $[jj']$ denotes a sum over nearest–neighbor oxygen pairs, and $\langle ij\rangle$ a sum over copper–oxygen nearest neighbors. In the d–p system we work in the hole representation so that $d^\dagger_{i,\sigma}$ ($p^\dagger_{j,\sigma}$) creates a hole on d (p) site i (j) with spin σ, and $n^d_{i\sigma}=d^\dagger_{i\sigma}d_{i\sigma}$ and $n^p_{j\sigma}$ are the local hole densities on a copper and oxygen site, respectively. The parameter t_{pp} is the strength of the direct hopping between the p-orbitals, Δ is the difference in on–site energies, U_p and U_d are the on–site Coulomb repulsion on the p and d sites respectively, t_{pd} is the hybridization and V_{pd} the Coulomb repulsion between nearest–neighbor p and d orbitals. The lattice structure of the d–p model including a schematic representation of the Hamiltonian parameters is shown in Fig. 1(a). Unless otherwise stated, we will consider lattices consisting of N copper sites and $N+1$ oxygen sites, with open boundary conditions at the ends of the lattice so that the ends consist of oxygen sites with connections in only one direction. When the system has N_h total holes, we will discuss $N_p\equiv N_h-N$, which corresponds to the excess number of holes in the oxygen band when $U_d>\Delta>0$, and the corresponding p–band filling, $n_p\equiv N_p/N$.

This model has a gauge symmetry which can be used to permute the signs of the hopping matrix elements around each triangular element. For example, alternating the sign of t_{pd} on succesive bonds and taking t_{pp} positive is equivalent to having the same sign of t_{pd} and taking t_{pp} negative. Here we take the latter case, as shown in Eq. (1), restrict t_{pd} to be positive, and allow the sign of t_{pp} to vary.

In order to understand the physics of ferromagnetism in the d–p model, it is useful to make a comparison with a model that has a similar structure in an appropriately chosen parameter regime, the one–dimensional periodic Anderson model. The PAM has Hamiltonian

$$H=-t\sum_{i\sigma}(c^\dagger_{i\sigma}c_{i+1\sigma}+c^\dagger_{i+1\sigma}c_{i\sigma})+\varepsilon_f\sum_{i\sigma}n^f_{i\sigma}+U\sum_i n^f_{i\uparrow}n^f_{i\downarrow}+V\sum_{i\sigma}(c^\dagger_{i\sigma}f_{i\sigma}+f^\dagger_{i\sigma}c_{i\sigma})\ , \tag{2}$$

where $c^\dagger_{i\sigma}$ and $c_{i\sigma}$ create and annihilate conduction electrons with spin σ at lattice site i, and $f^\dagger_{i\sigma}$ and $f_{i\sigma}$ create and annihilate local f–electrons. Here t is the hopping matrix element for conduction electrons between neighboring sites, ε_f is the energy of the localized f–orbital, U is the on–site Coulomb repulsion of the f–electrons, and V is the on–site hybridization matrix element between electrons in the f–orbitals and the conduction band. We denote the number of electrons by N_e, and N is the number of unit cells (each consisting of one f site and one conduction site) in the lattice. Since there are two electronic orbitals in each site, the quarter–filled case corresponds to $N_e = N$ and the half–filled case has $N_e = 2N$. In analogy to the d–p model, we will discuss $N_c = N_e - N$, the excess number of electrons in the conduction band when $U > -\varepsilon_f > 0$, and the corresponding filling, $n_c \equiv N_c/N$. Fig. 1(b) shows a schematic represention of the PAM.

One can set the parameters of d–p model so that it is the same as the PAM except that the d-orbital hybridizes with the two nearest–neighbor copper atoms, while the PAM hybridizes only on–site. In order to compare the two models, we set $V_{pd} = U_p = 0$, $t_{pp} = t$, $t_{pd} = V$, $\Delta = -\epsilon_f$ and $U_d = U$.

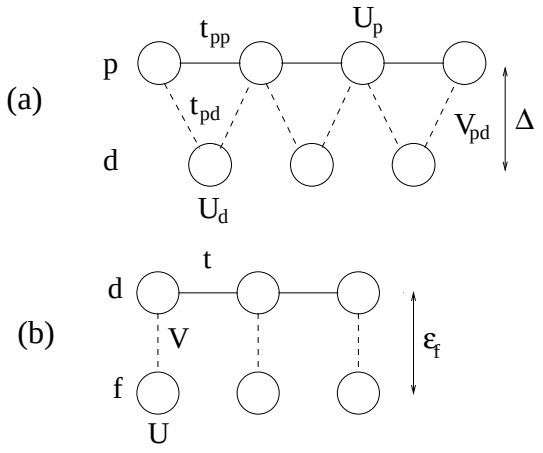

FIG. 1. A schematic diagram of (a) the copper–oxide lattice and (b) the periodic Anderson model, with the system parameters marked.

III. CALCULATION AND RESULTS

Since itinerant ferromagnetism is an intrinsically strong–coupling phenomenon that occurs due to a subtle competition between kinetic and potential energy,[3] it is generally quite hard to treat with analytic methods. While exact statements can be made in some special cases, such as the Nagaoka state[19] and the case of flat bands,[6] in general one must resort to mean–field theory or variational techniques, both of which give phase diagrams which can be at best qualitatively accurate. Therefore, sufficiently accurate numerical methods can be useful to determine the properties of models with ferromagnetic phases. Here we use the Density Matrix Renormalization Group to calculate the ground–state properties of the d–p model and the PAM. The DMRG is a variational numerical method closely related to exact diagonalization, but which can be used to treat much larger systems.[20,21] Being able to treat sufficiently large systems is important since the models we study here have two fermionic sites, i.e. sixteen degrees of freedom per unit cell, which would severely limit the maximum size available for exact diagonalization. Quantum Monte Carlo methods would suffer from the fermion sign problem at all band fillings on the d–p lattice.

We use the finite–system version of the ground–state DMRG algorithm[20] to accurately calculate the energy expectation values of equal–time operators in the ground state including local spin, density, and various correlation functions. We keep up to 800 states in the system block and treat lattices of up to $N = 32$ unit cells. The maximum sum of discarded density matrix eigenvalues is approximately 5×10^{-6}.

In order to search for ferromagnetic phases, it is essential to be able to determine the total spin of the ground state. Since our version of the DMRG algorithm does not allow direct control of the total spin, we use a combination of methods to do this. First, we can calculate the expectation value $\langle\psi_0|S^2|\psi_0\rangle$ directly, where ψ_0 is the variational DMRG ground state calculated in a particular S_z sector, and S^2 is the explicit operator for the square of the total spin. Since the DMRG ground state is variational, $\langle\psi_0|S^2|\psi_0\rangle$ does not always take on the quantized values due to mixing between states of different S_z. Second, we can add a term of the form λS^2 to the Hamiltonian, raising the energy of higher spin states within a particular S_z sector.[4] We can use this to calculate the ground–state energy as a function of S^2 by examining the energy of the minimum S^2 ground state in a particular S_z sector. Finally, we can examine the ground–state energies as a function of S_z and use the degeneracy in S_z to determine S^2. For application of these methods to the ferromagnetism in the PAM, see Ref. 12 and to the Hubbard chain with next–nearest–neighbor hopping, see Ref. 4.

A. Comparison with the periodic Anderson model

In the first part of this work, we present a comparison between the d–p system and the PAM. The qualitative picture developed for the ferromagnetic phase of the PAM[22,12] should also apply to the d–p model. In order to make the correspondence to the PAM, we choose a regime in which the d-orbital lies below the bottom of the p-band. At exactly quarter filling, all the electrons are in the d-sites and all the spin states are degenerate if there is no hybridization. When the hybridization is turned on, the super-exchange favors antiferromagnetic interactions. The exchange coupling constant can be calculated

from perturbation theory giving

$$J_A = \frac{4t_{pd}^4}{(\Delta + V_{pd})^2}\left(\frac{1}{U_d} + \frac{2}{2\Delta + U_p}\right) , \qquad (3)$$

or when $U_d = 2\Delta$ and $U_p = V_{pd} = 0$, $J_A = 6t_{pd}^4/\Delta^3$. When a hole is added to the quarter–filled system, it will prefer to go to the p-sites since $U_d > |\Delta|$. This extra hole will tend to form singlets with the mostly localized spins in the d-sites. The hole can delocalize and thus lower its energy if the spins of the d–holes are oriented in the same direction, i.e. are ferromagnetically ordered. The binding energy for these singlets can be calculated within perturbation theory in a manner similar to that applied to the two-dimensional case by Zhang and Rice,[23] yielding

$$J_S = 2t_{pd}^2\left(\frac{1}{\Delta - V_{pd}} + \frac{1}{\Delta - V_{pd} + U_p} + \frac{2}{U_d - \Delta - V_{pd}}\right) . \qquad (4)$$

For $U_d = 2\Delta$ and $U_p = V_{pd} = 0$, $J_S = 8t_{pd}^2/\Delta$.

In general, when there are $N_p = N_h - N$ holes in the p-band, this effect will favor a ferromagnetic ground state with total spin $S = (N - N_p)/2$. We will denote this value of S for the ground state as *complete* ferromagnetism, while a value of S smaller but still greater than the minimum, will be labeled *incomplete*. Note that a complete state has a lower magnetization than a saturated one. It represents a state where all the *uncompensated* d-spins are aligned.

Thus, one would expect a competition between ferromagnetism and antiferromagnetism near quarter filling similar to that found in the PAM.[12] For the PAM there is an exact result that proves the ground state is ferromagnetic with complete magnetization for $N_c = 1$ ($N_e = N + 1$) and $U_d = \infty$.[24,25] There is no such result, however, for the d–p model. Furthermore, while the antiferromagnetic exchange is a sixth–order process in the Anderson lattice model, it is fourth order (and therefore stronger) in the d–p system. Therefore, it is not clear that the ferromagnetism will still be present in the d–p system. Yanagisawa[25] studied a 2×2 CuO cluster with exact diagonalization and found a ferromagnetic ground state. However, it is difficult to draw general conclusions about the behavior in the thermodynamic limit from such a small cluster.

In our DMRG calculations, we consider chains with $N = 16$ and open boundary conditions and set $t_{pp} = 0.5$, $t_{pd} = 0.375$, $\Delta = U_d/2$ and $U_p = V_{pd} = 0$. This choice allows us to compare the phase diagram with the one of the Anderson lattice model from Ref. 12 where $t = 0.5$, $V = 0.375$, $\epsilon_f = -U/2$. In Fig. 2, we present both phase diagrams in the plane of band filling and the local Coulomb repulsion, U or U_d. Here $n_c = 0$ ($n_p = 0$ for the d–p model) represents the quarter-filled case, which in the large Coulomb repulsion regime means that the localized orbitals are singly occupied and the extended orbitals are empty in the zero hybridization limit. In the d–p system, Fig. 2(b), the region of complete ferromagnetism is pushed towards higher values of U_d and higher densities and there is a wide region of incomplete states at low densities. This is consistent with the fact that antiferromagnetic correlations at quarter filling in this system are of lower order (and therefore stronger) than in the Anderson lattice model.

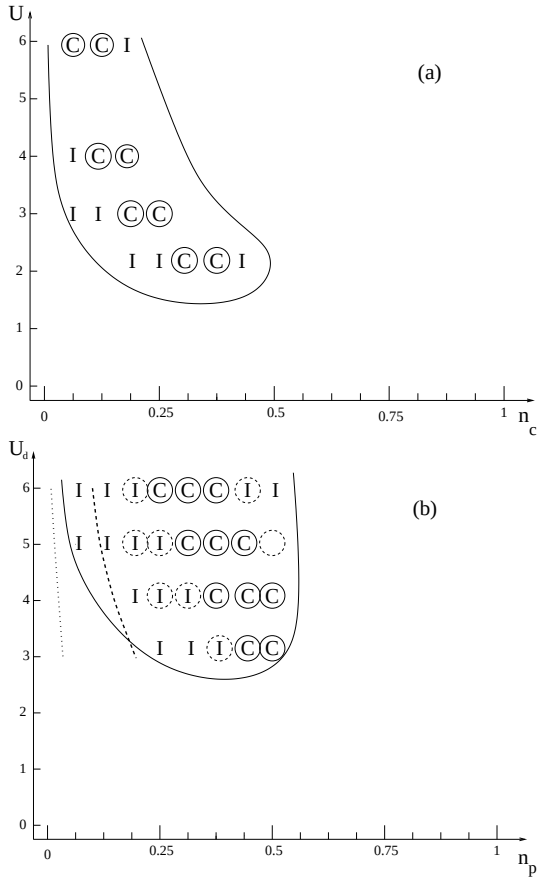

FIG. 2. Ground–state phase diagram in the plane of band filling and the local Coulomb repulsion for an $N = 16$ system of (a) the Anderson lattice with $V = 0.375$, $t = 0.5$, $\epsilon_f = -U/2$, and (b) the copper–oxide lattice with equivalent parameters: $t_{pd} = 0.375$, $t_{pp} = 0.5$, $\Delta = U_d/2$, $U_p = V_{pd} = 0$. At $n_c = 0$ or $n_p = 0$, each system is quarter–filled, i.e. has one hole per unit cell. The dotted and dashed lines in (b) correspond to Eq. (5) and Eq. (11), respectively.

In Fig. 3 we show the Cu–Cu correlation function, $\langle S_d^+(r) S_d^-(0)\rangle$, as a function of distance, r (measured in units of the lattice constant), for the d–p model with the parameters described above and $U_d = 5$ for $N_p = 0$, 2 and 4. Here $S_d^+(r) = d_{r,\uparrow}^\dagger d_{r,\downarrow}$ is the d–spin raising operator on site r. For $N_p = 0$ (quarter filling), the correlations are clearly antiferromagnetic with the amplitude decay-

ing slowly with distance, while for $N_p = 2$ and $N_p = 4$, the correlations are ferromagnetic. This illustrates that the system goes from an antiferromagnetic state at quarter filling to a ferromagnetic state as soon as additional holes are added for these parameter values.

The competition between the tendency to ferromagnetism and the antiferromagnetic exchange gives rise to the region of *incomplete* ferromagnetism at low doping. In this region, we find that the system *phase separates* into domains of complete ferromagnetism in which the p–holes are localized and antiferromagnetic domains in which the p–band is empty. Indeed, the first symptom of this phase separated state can be seen in Fig. 3, in which there is a jump in the correlation function for $r = 12$ for the case of 18 holes. This peculiar behavior is due to the tendency of the holes to localize and form a region of complete ferromagnetism near the center of the chain, leaving the p-orbitals empty near the ends.

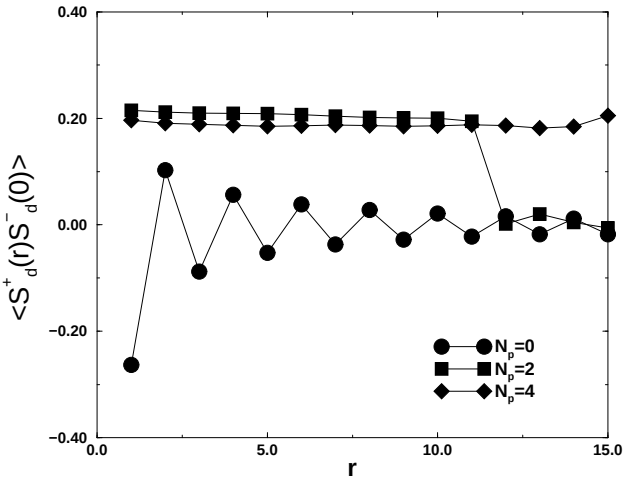

FIG. 3. The Cu–Cu spin–spin correlation function as a function of distance, r, for the copper–oxide lattice with the same parameters as in Fig. 2 and $U_d = 5$ for 3 different fillings.

To illustrate this phase–separated regime, we have calculated the chemical potential $\mu = E_o(N_h+1) - E_o(N_h)$, where $E_o(N_h)$ is the ground state energy with N_h holes, for chains of $N = 8$, 16 and 32 unit cells. We show μ as a function of the filling for $U_d = 5$ in Fig. 4. For 8 unit cells, μ increases monotonically with n_p, but for 16 unit cells there is a shallow minimum at $n_p = 0.0625$. For 32 unit cells, there is a flat region which is shown in detail in the inset, with a minimum at $n_p = 0.09375$ which is indicative of phase separation. We find a similar behavior of the chemical potential is found for $U_d = 6$ and $U_d = 4$.

To illustrate the localization of the holes in the p–band, we display the density in the p–sites as a function of position in the lattice for $U_d = 4$ in an $N = 32$ unit–cell chain with $N_p = 0, 1, 2, 3$ in Fig. 5. At quarter filling, the p–levels are almost empty. Upon doping, they begin to fill with holes, but instead of spreading out over the lattice, the additional holes localize in a region which is smaller than the lattice size. This behavior is also seen for $U_d = 5$ and $U_d = 6$.

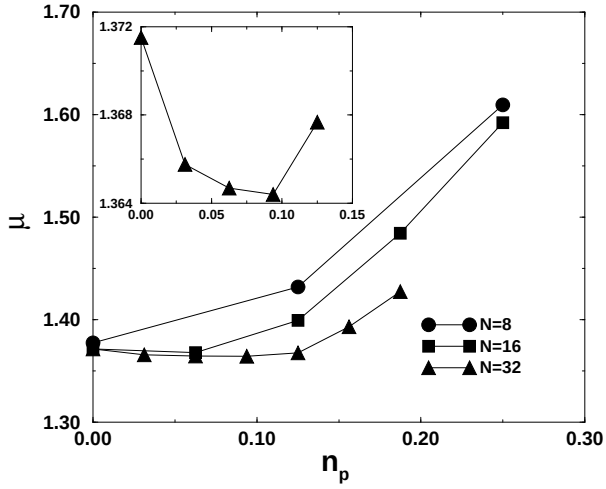

FIG. 4. The chemical potential μ, as a function of the p–band filling, n_p, for the Cu-O lattice with the same parameters as in Fig. 3 for different system sizes. The inset is an expanded view of the low–density results for the 32 unit–cell lattice showing a minimum in the chemical potential, the signature for phase separation.

In Fig. 6 we show the local spin density $\langle S_i^z \rangle$ as a function of position in the lattice for an $N = 32$ chain with $U_d = 5$, $N_p = 2$ and $S_z = S = 5$ (the ground state) for both the p–band and the d–band. There are two distinct domains in the lattice: one in which the d–holes are completely polarized and another one in which they tend to order antiferromagnetically. The coupling between p and d holes is clearly antiferromagnetic. The asymmetry of the distribution is a numerical artifact due to the near–degeneracy of states with the phase–separated region centered at different points.

To gain some physical insight into the phase separation mechanism, one can use energetic arguments to estimate the stability of competing phases. The energy scale in the antiferromagnetic state is set by J_A, the antiferromagnetic exchange energy, Eq. (3). The energy of the uniform ferromagnetic phase can be estimated by the binding energy of the Zhang–Rice–like singlets, $J_S N_p$. For a rough estimate of the magnetic energy scale, consider an antiferromagnetically ordered state versus one that has complete ferromagnetism. The Bethe Ansatz energy of a one–dimensional Heisenberg antiferromagnet[26] consisting of $N-1$ bonds (measured relative to the ferromagnetic state and neglecting end effects) is $J_A^{\rm eff}(N-1)$, where $J_A^{\rm eff} = \ln 2 J_A$. In order for complete ferromagnetism to occur, the condensation energy of the singlets, $J_S N_p$ must be larger than this, leading to the condition

$$n_p \gtrsim \ln 2 J_A / J_S \equiv n_{pc1} \ . \qquad (5)$$

This estimate is only valid for very low densities of p–electrons, since it neglects their kinetic energy, and for

strong coupling where the magnetic picture is valid. According to this estimate, ferromagnetism is favored over antiferromagnetism for $U_d \gtrsim 3$ at all densities above quarter-filling on the lattice sizes that we have studied. However, it yields a smaller n_{pc1} than we find in the numerical calculations. For example, for $U_d = 4$ and the parameter set used in this section, $n_{pc1} = 0.018$.

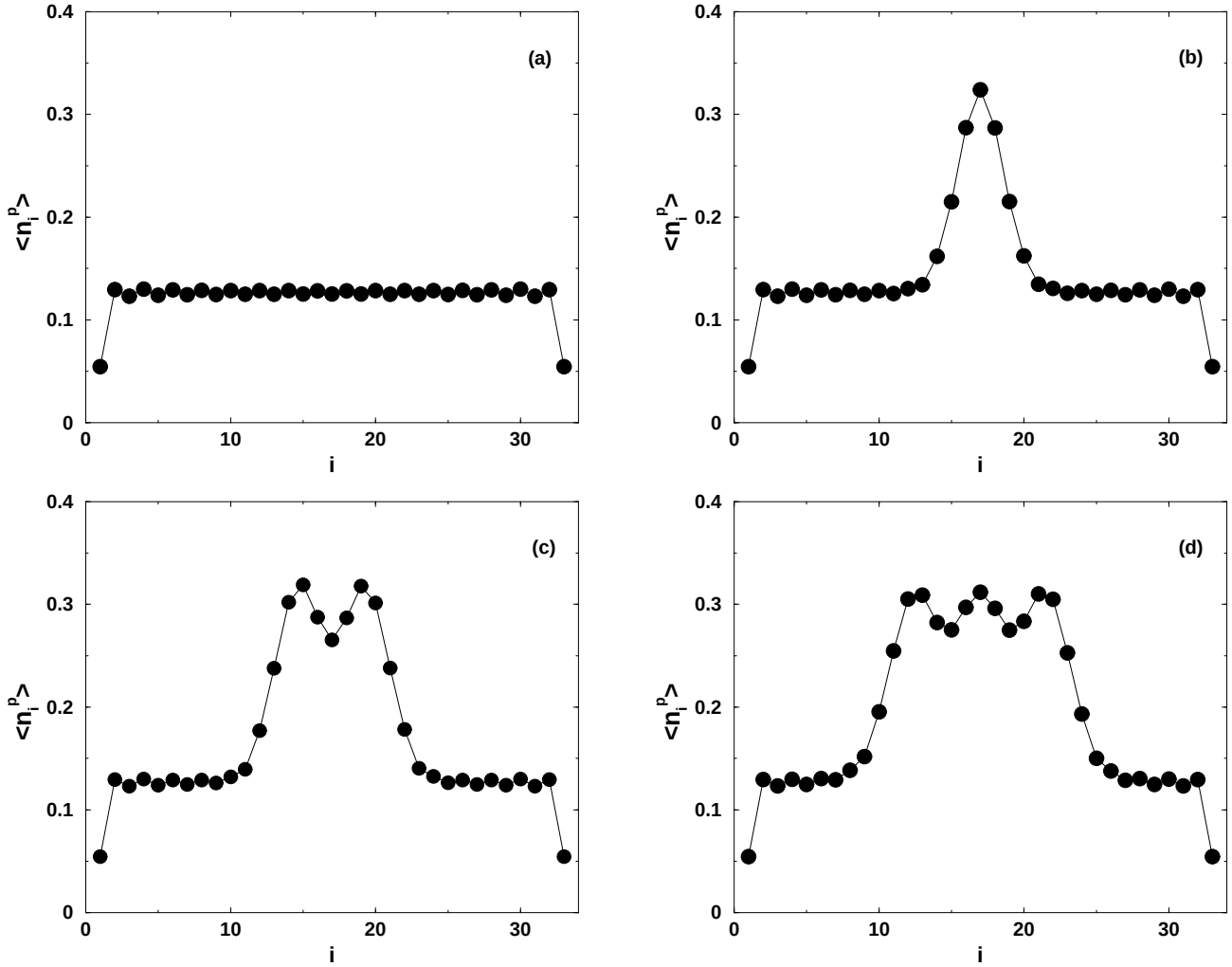

FIG. 5. Density in the oxygen sites as a function of position in the lattice, i, with $N = 32$ unit cells, the same parameters as in Fig. 2 and $U_d = 4$ for (a) $N_p = 0$ (quarter filling), (b) $N_p = 1$, (c) $N_p = 2$, and (d) $N_p = 3$.

Now let us examine the possibility of phase separation between a region of undoped antiferromagnetism and a region of complete ferromagnetism. In order for such a phase to exist, the energy gained by forming an undoped antiferromagnetic domain must compensate the loss in kinetic energy of the Zhang–Rice singlets, which have to localize in a region smaller than the lattice size N. We estimate the kinetic energy of the Zhang–Rice singlets by taking them to be noninteracting hard–core bosons confined to a lattice of length X with open boundary conditions. (We study lattices with open boundary conditions here, so that this form is valid up to the number of p–sites, $X = N + 1$.) The single–particle energy levels are given by

$$\varepsilon_j = -2t_{ZR} \cos \frac{\pi j}{X+1} \ , \tag{6}$$

where t_{ZR} is the effective hopping of the singlets and $j = 1, \ldots, N$. Since hard–core bosons are equivalent to spinless fermions in one dimension, the total kinetic energy is given by successively occupying single–particle states,

$$\begin{aligned} T(N_p, X) &= \sum_{j=1}^{N_p} \varepsilon_j \\ &\approx \int_0^{N_p} dj \ \varepsilon_j \approx -2t_{ZR} \ \frac{X}{\pi} \ \sin \frac{N_p \pi}{X} \ , \end{aligned} \tag{7}$$

where the approximation on the right–hand side is valid in the continuum limit: $X \gg 1$. The energy gained by constricting the ferromagnetic domain to a length X is

$$E_{PS}(N_p, X) = J_A^{\rm eff}(N-1-X) + T(N_p, N+1) - T(N_p, X) \; . \qquad (8)$$

The phase–separated state will be favored over the homogeneous ferromagnetic state if E_{PS} is positive. In that case, the size of the ferromagnetic region is given by the value of X that maximizes the energy gain, determined by

$$0 = \frac{\partial E_{PS}}{\partial X} \approx -J_A^{\rm eff} + \frac{2\pi^2 t_{ZR} N_p^3}{3X^3} \; , \qquad (9)$$

where we have taken $N_p\pi \ll 1$ in order to expand the sine and have used the continuum expression from the right–hand side of Eq. (7). Eq. (8) has one maximum for $X > 0$ which occurs at

$$X_{\rm max} = N_p \left(\frac{2\pi^2 t_{ZR}}{3J_A^{\rm eff}} \right)^{1/3} \equiv N_p x_o \; . \qquad (10)$$

It is easy to verify that $E_{PS}(N_p, X_{\rm max})$ is always positive as long as $0 < X_{\rm max} < N$. Therefore $X_{\rm max}$ is the length of the ferromagnetic domain when phase separation is present. Note that $X_{\rm max} \propto N_p$, in agreement with the behavior seen in Figs. 5 and 6. In order to numerically estimate x_0 for the d–p system, we take $t_{ZR} = t_{pp}$ and $J_A^{\rm eff} = \ln 2 J_A$, where J_A is given by Eq. (3) for the d–p model. (One could calculate t_{ZR} more accurately in perturbation theory, but only its order of magnitude is important, since it appears within the cube root.) For the parameters used in this section, this gives $x_0 = 7$, 8.5 and 10 for $U_d = 4$, 5 and 6, respectively. This is in reasonable agreement with our numerical results (See Fig. 5), which also show an increase in the localization length with U_d.

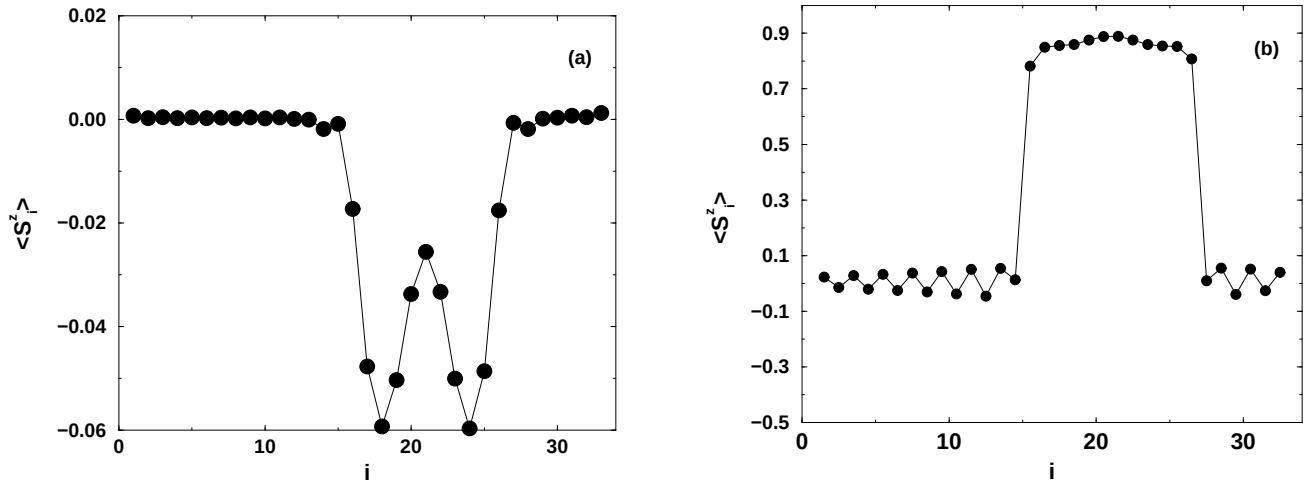

FIG. 6. The local spin density $\langle S_i^z \rangle$ as a function of lattice position, i, for (a) the oxygen sites and (b) the copper sites on an $N = 32$ lattice with $S_z = S = 5$ (the ground state) and $N_p = 2$. Here $U_d = 5$ and the remaining parameters are the same as in Fig. 2.

The boundary between the uniform ferromagnetic phase and the phase–separated phase is determined by the condition $X_{max} = N$, leading to a critical density

$$n_{pc2} = \left(\frac{3J_A^{\rm eff}}{2\pi^2 t_{ZR}} \right)^{1/3} \; . \qquad (11)$$

The densities n_{pc1} and n_{pc2} calculated from Eqs. (5) and (11) are represented in the phase diagram of Fig. 2(b) as dotted and dashed lines, respectively. Notice that the numerical calculation yields a somewhat wider region of phase separation than given by these estimates. In order to estimate the finite–size effects, we have also examined the spin of the ground state on $N = 8$ and $N = 32$ unit–cell chains. We find that the points of complete polarization in Fig. 2(b) behave consistently with system size, i.e. are also completely polarized for $N = 8$ and $N = 32$. However, the scaling behavior of the incomplete states is more complicated. In particular, some states which are incompletely polarized in the $N = 16$ chain become completely polarized for $N = 32$. These cases are circled with a dashed line in Fig. 2(b). Therefore, the phase–separated region tends to become narrower in the thermodynamic limit. There is, however, evidence that some of the incompletely polarized states remain in the thermodynamic limit. For $U_d = 5$ and 6, the two densities closest to quarter filling on the $N = 16$ chain have total spin $S = 5/2$ and 5, and $S = 7/2$ and 6, respectively. On the $N = 32$ chain, the ground–state S at the same density doubles, suggesting that S/N will remain constant in the thermodynamic limit. At $U_d = 4$ and $U_d = 3$, none of the incomplete states show such a simple scaling and we

believe that larger system sizes are needed to determine the nature of the phase boundaries. For $U_d = 3$, we find no evidence of phase separation at any finite system size.

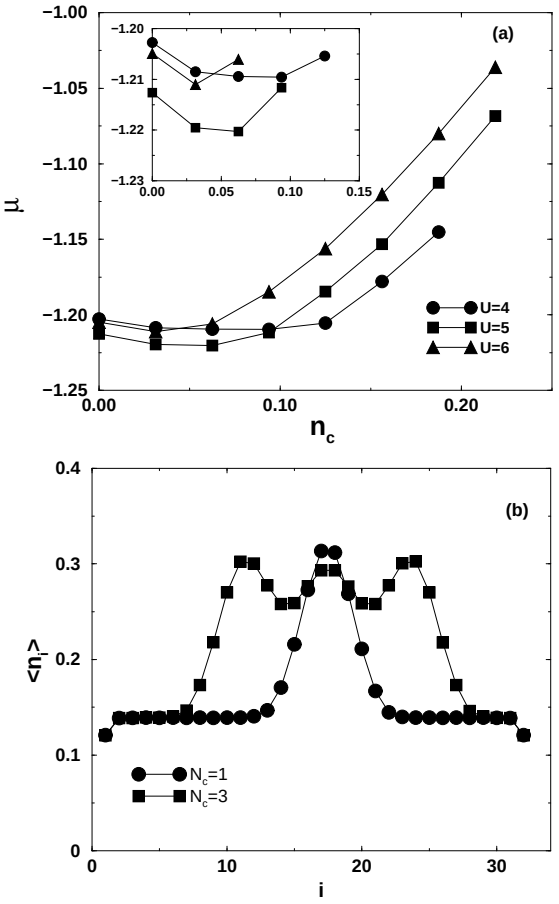

FIG. 7. (a) The chemical potential, μ, versus density, n_c, for the periodic Anderson model with $V = 0.75$, $t = 0.5$, and $\epsilon_f = -U/2$ on an $N = 32$ lattice. It shows a minimum for all three U–values. (b) Conduction electron density versus site for the $U = 5$ case, showing localization of the excess conduction electrons in a region smaller than the lattice size.

Let us now examine the relevance of the phase separation arguments to the PAM. Our energetic arguments should also apply with the appropriate mapping of J_A and J_S to the model parameters. For the symmetric case, $\varepsilon_f = -U/2$, $J_S = 8V^2/U$ and $J_A = 8V^4t^2/\varepsilon_f^5$. For the parameter sets we have compared on the two models, J_A is smaller in the PAM than in the d–p system. This implies that phase separation occurs over much larger localization lengths in the PAM. Indeed, for the conduction electron density $n_c = 1/32$ we obtain $x_o \approx 28$, 21 and 14 for $U = 6$, 5 and 4, respectively. Because these lengths are larger than those for the $d - p$ system, we could not find definite numerical evidence of a phase–separated state on the lattice sizes that we were able to study; larger systems sizes would be required. In order to confirm our picture of the origin of the phase separation, we can instead reduce x_0 by increasing the hybridization V; we double V to $V = 0.75$, decreasing the localization length by a factor of two to $x_o \approx 14$, 10 and 7 for $U = 6$, 5 and 4, respectively. Using the DMRG, we then examine $N = 32$ systems with $t = 0.5$, $\epsilon_f = -U/2$ and $V = 0.75$ for $U = 4$, 5, and 6. The results, presented in Fig 7, show numerical evidence for phase separation for all three U–values. The chemical potential, Fig. 7(a), has a minimum as a function of the filling, and the conduction electron density, Fig. 7(b), tends to localize in a region smaller than the size of the system. Therefore, we find that phase separation can also occur in the PAM under the right conditions.

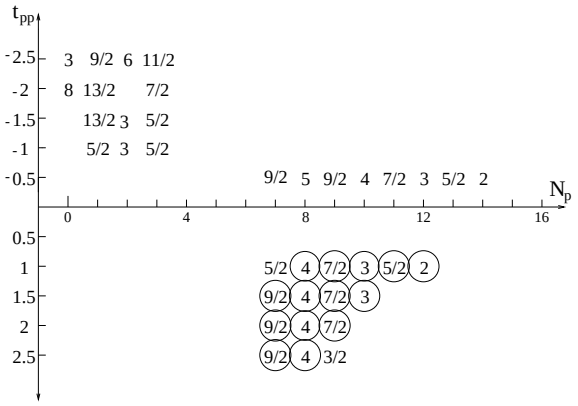

FIG. 8. Phase diagram in the plane of oxygen occupation, N_p, and hopping t_{pp} for an $N = 16$ copper–oxide lattice with $t_{pd} = 1$, $U_d = 8$, $\Delta = 3$, $U_p = 4$, $V_{pd} = 0.5$. The total spin, S, has been calculated everywhere in the plane, but is shown as a numerical value only when it is greater than the mimimum value, $S = 0$ for even or $S = 1/2$ for odd N_p. Cases of "complete" polarization are circled.

B. Phase Diagram for "Realistic" Parameters

In the second part of our work, we think of the d–p system as the one–dimensional analog of the copper–oxide planes in high temperature superconductors. We set the parameters $t_{pd} = 1$, $U_d = 8$, $U_p = 4$, $\Delta = 3$ and $V_{pd} = 0.5$, values reasonable for the cuprates,[27] and then vary t_{pp} and the hole filling. The resulting phase diagram is shown in Fig. 8 for an $N = 16$ chain and both possible signs of t_{pp}. The cases with complete polarization, $S = (N - N_p)/2$, are circled. For $t_{pp} > 0$ the phase diagram has one ferromagnetic region consisting almost exclusively of complete polarization for $t_{pp} > 1$ and from $n_p \sim 0.4$ to $n_p \sim 0.75$. The arguments of the first part of our work should also apply to this region, i.e. the ferromagnetic ordering of the f–spins is caused by the condensation of Zhang–Rice singlets. As can be seen from the lack of regions of incomplete polarization, we find no phase separation at these parameter values. It is clear that Eq. (5) cannot properly predict the boundary of the ferromagnetic phase since it is invalid at the

relatively large N_p values at which we find the phase. From Eq. (10), the charactistic size of the localization of the singlets is given by $x_0 \approx 4.5\ t_{pp}^{1/3}$ for these parameter values. Our energetic arguments therefore predict no phase separation at the densities at which we do find a ferromagnetic phase.

When $t_{pp} < 0$ the phase diagram is quite different. There is one point at quarter filling and $t_{pp} = -2$ for which the ground state is fully polarized ($S = 8$ for $N = 16$), surrounded by a region of smaller polarization. Additionally, there is a region with polarization greater than complete, but less than fully polarized for a narrow range of t_{pp} but a wide range of hole occupation, N_p. More precisely, the extent of this region is $-0.5 \lesssim t_{pp} \lesssim -0.7$ and $7 \leq N_p \leq 14$.

We first discuss the fully polarized phase at quarter filling and $t_{pp} \approx -2.0$. One can gain insight into the origin of this ferromagnetic phase by examining the noninteracting band structure. Diagonalization of the Hamiltonian, Eq. (1), with $U_d = U_p = V_{pd} = 0$ and periodic boundary conditions leads to the hybridized bands

$$\varepsilon_{\pm}(k) = \Delta/2 - t_{pp}\cos k \pm \sqrt{(\Delta/2 - t_{pp}\cos k)^2 + 2t_{pd}^2(1+\cos k)}\ . \tag{12}$$

These bands, plotted for three t_{pp} values near the fully polarized point, are shown in Fig. 9. As can be seen, the lower band does not overlap with the upper band and has a dispersion that is quite flat; it becomes completely flat at $t_{pp} = -1.78$. Therefore, all the holes will go into the half–filled flat band at this point. A theorem by Mielke,[6] subsequently extended to nearly flat bands by Mielke and Tasaksi[7] shows rigouously that for the Hubbard model with a low–lying completely flat band at half–filling or less will have a fully polarized ground state. Therefore, this region is due to flat–band ferromagnetism. This is substantiated by the strong dependence of the polarization on t_{pp} and n_p; there is only a small region of partial polarization surrounding the fully polarized point.

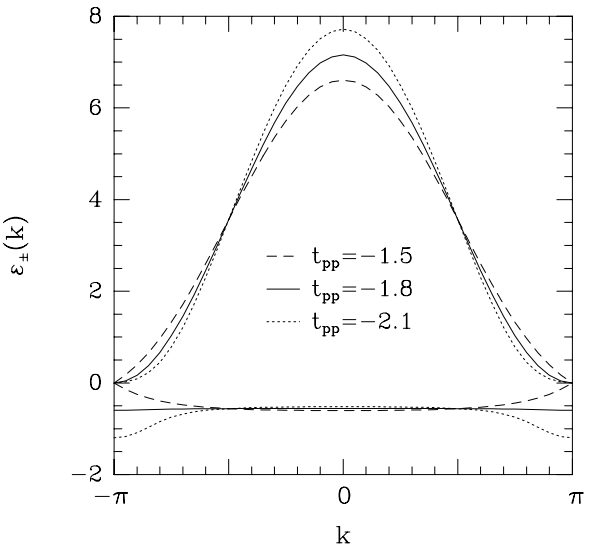

FIG. 9. The dispersion of the non-interacting bands, $\varepsilon_{\pm}(k)$, of the d–p lattice for $t_{pd} = 1.0$, $\Delta = 3.0$ and three different t_{pp}.

We next treat the narrow strip of ferromagnetism at $t_{pp} \approx -0.5$ and intermediate N_p. The first important issue is whether the partial polarization in this region persists in the thermodynamic limit. In Fig. 10, we plot S/N as a function of $1/N$ for three different fillings. As can be seen, S/N increase linearly with $1/N$ and extrapolates to a finite value as $N \to \infty$.

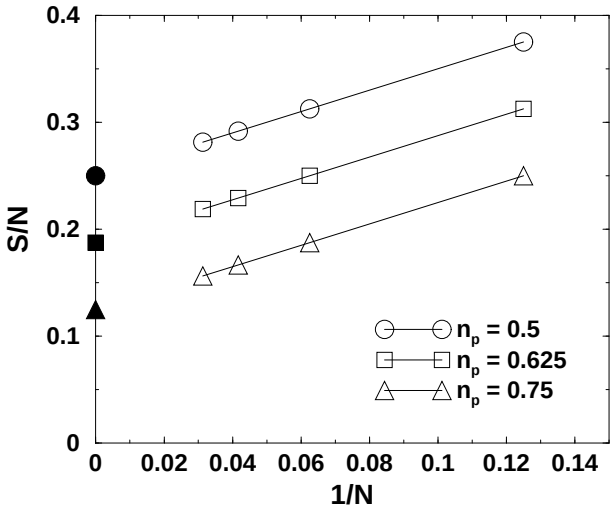

FIG. 10. Total spin per site, S/N, as a function of $1/N$ for a copper–oxide lattice with the same parameters as in Fig. 8, $t_{pp} = -0.5$ and three different fillings. The corresponding solid symbols show the $N \to \infty$ values obtained from a linear extrapolation in $1/N$.

One can gain some insight into the relationship between the sign of t_{pp} and the mechanism for ferromagnetism by examining the behavior of small clusters. In particular, we examine the behavior of one triangular element of the lattice, i.e. a cluster consisting of one copper and two oxygen sites, occupied by two holes ($N = 1$, $N_p = 1$). This CuO_2 cluster can be treated analytically if spin and reflection symmetry are taken into account: The total spin can either be zero or one, and states can be symmetric and antisymmetric with respect to exchange of the oxygens. The antisymmetric $S = 0$ and the symmetric $S = 0$ sectors can be represented by 2×2 matrices, the symmetric $S = 0$ sector is 4×4, and the antisymmetric $S = 1$ sector is 1×1. All of these matrices can be di-

agonalized analytically (although it is easier, in practice, to treat the 4×4 matrix numerically since the general solution is rather complicated). Taking $t_{pd} = 1$, $U_d = 8$, $U_p = 4$, $\Delta = 3$ and $V_{pd} = 0.5$, and varying t_{pp}, we find that for $t_{pp} > 0$, the ground state is always a singlet with positive reflection symmetry. For $t_{pp} < 0$, there is a competition between singlet formation, favored by direct antiferromagnetic exchange, and triplet formation, favored by third order exchange around the plaquette, which is ferromagnetic.

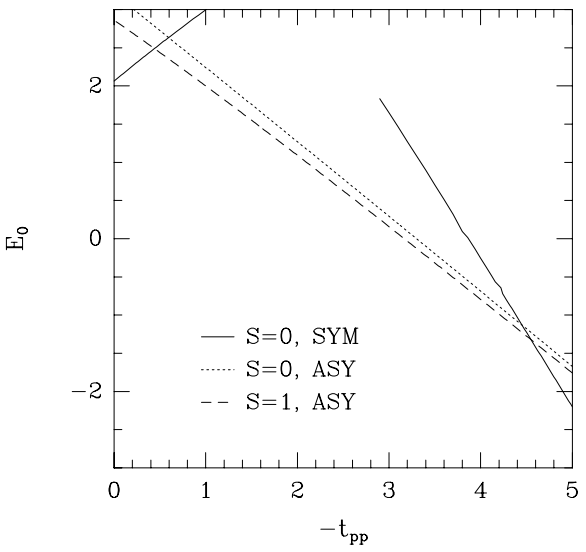

FIG. 11. The energies of the three lowest lying states of the CuO_2 cluster for $t_{pd} = 1$, $U_d = 8$, $U_p = 4$, $\Delta = 3$ and $V_{pd} = 0.5$, as a function of $-t_{pp}$. Here "SYM" denotes a state that is symmetric with respect to exchange of the oxygens, and "ASY" denotes an antisymmetric state.

In Fig. 11, we show the dependence of the energy of the three lowest lying states of the CuO_2 cluster on $-t_{pp}$. As can be seen, for $0 < -t_{pp} \lesssim 0.46$ and $-t_{pp} \gtrsim 4.5$, the ground state is a singlet with positive reflection symmetry. In the intermediate range, $0.46 \lesssim -t_{pp} \lesssim 4.5$, the ground state is an antisymmetric triplet, which is close in energy to the first excited state, an antisymmetric singlet. This illustrates the effect of the sign of t_{pp} on the basic triangular element of the lattice: a localized triplet is only possible for negative t_{pp} and can occur only for a certain range of $-t_{pp}$, when there are two holes on the plaquette.

While the triplet ground state of the CuO_2 cluster motivates the possibility of a ferromagnetic state in this region, and provides an explanation for the minimum value of $-t_{pp}$ required, it cannot provide a complete picture of this phase. In particular, the range of $-t_{pp}$ with a triplet ground state is much wider in the CuO_2 cluster than the range of $-t_{pp}$ in the ferromagnetic strip in Fig. 8. When more triangles are connected together, interaction between holes in the p–band can become important. The point of maximum polarization occurs when $n_p \approx 0.5$, i.e. there is one hole for every second p–site. At this filling, ferromagnetism based on exchange around the triangular elements would be somewhat frustrated since each p–site is shared by two triangular elements. These mechanisms would tend to suppress ferromagnetism. Also, as seen in Fig. 11, the triplet ground state is close in energy to a singlet excited state even on a single triangular element.

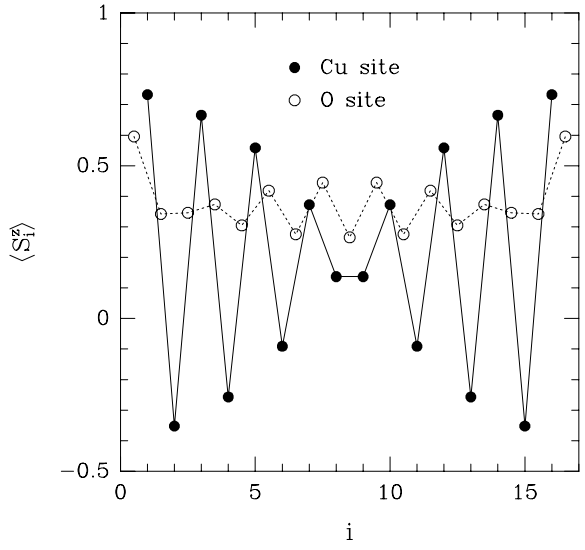

FIG. 12. Local spin density $\langle S_i^z \rangle$, as a function of Cu–site index i for both the copper (Cu) and oxygen (O) sites on an $N = 16$ d–p lattice with $N_p = 8$ ($n_p = 0.5$), $t_{pp} = -0.6$, $S_z = 5$ and the remaining parameters as in Fig. 8. For the oxygen sites, i takes on half-integer values between the corresponding Cu–sites.

We can gain additional insight into these effects from diagonalization on clusters larger than three sites. For clusters of $N = 2$, 3, and 4 unit cells (5, 7, and 9 total sites) with open boundary conditions, a ferromagnetic ground state appears at all fillings in the range $0 < N_p \leq N$ for $-t_{pp} \gtrsim -t_{pp}^{\min}$, with $t_{pp}^{\min}$ ranging from -0.52 to -0.48. However, the extent of this region in t_{pp} and the value of the polarization depends on N_p. For $N_p = 1$, one hole in the p–band, and all three sizes, we obtain a ground–state spin at or close to the maximum possible value, up to $t_{pp}^{\max}$ ranging between -2.9 and -4.2. This behavior is like that in the $N = 1$ CuO_2 cluster, since all the d–holes are ferromagnetically polarized. It is also reminiscent of the ferromagnet phase in the PAM, except that it is a triplet state which delocalizes rather than a singlet. Similar ferromagnetic states have been found in the one-dimensional Kondo lattice model with ferromagnetic exchange.[28]

For larger N_p, we obtain a ferromagnetic ground state up to $t_{pp}^{\max}$ ranging from -0.62 to -0.70, a value in good agreement with that found in larger systems. The

ground–state spin varies and depends on N_p. One can understand the nature of this phase by examining the distribution of spin polarization and the spin–spin correlation function. We display the local spin polarization, $\langle S_i^z \rangle$, for parameters that yield the maximum polarization on a $N = 16$ cluster in Fig. 12, taking $S_z = 5$, the maximal value. One can see that the holes on the d–sites are *antiferromagnetically* aligned, which we have confirmed by examining the spin–spin correlation function. The p–sites, however, all have positive polarization, and are ferromagnetically correlated with the positively polarized d–sites, i.e. with every other d–site. The correlations between p–sites are generally ferromagnetic. The picture is then that there is an alternation between triangular plaquettes with a ferromagnetic moment and isolated d–holes antiferromagnetically aligned with the neighboring plaquettes. This phase is reminiscent of a ferrimagnet with alternating $S = 1/2$ and $S = 1$. Changing the band filling can frustrate this order, changing the amount of polarization. One domain wall is visible in Fig. 12. Since this phase is due to a subtle competition between ferromagnetic and antiferromagnetic exchange processes, it is not surprising that it is quite sensitive to the value of t_{pp}. Certainly the picture of localized plaquettes breaks down as the hopping between the p–sites increases.

IV. CONCLUSIONS

We have studied ferromagnetism in the phase diagram of the one dimensional d–p model. In the first part of this work, we have compared the phase diagram near quarter filling of a d-p system to the one-dimensional periodic Anderson model. In both cases, we have found a ferromagnetic region near quarter filling, but, for equivalent values of the parameters, the ferromagnetic region in the d–p system is pushed towards higher values of the Coulomb interaction and higher densities.

Between the antiferromagnetic state at quarter filling and the homogeneous ferromagnetic region, there is a phase-separated regime in which ferromagnetic domains are segregated from the antiferromagnetic background. The phase–separated state arises because the loss of kinetic energy of the holes due to their localization in a small region is compensated by the gain in antiferromagnetic bonds. This regime is more evident in the d–p system because the antiferromagnetic coupling is stronger than in the Anderson model and therefore the characteristic length for the ferromagnetic domains is smaller. Nevertheless, we have presented numerical evidence for the phase–separated state for both models.

Recently, similar phases with a hole-rich ferromagnetic domains segregating from hole-undoped antiferromagnetic regions have been reported for models such as the one-orbital ferromagnetic Kondo model and other models studied in relation with manganites. (See Ref. 28 and references therein.) In our case, it must be emphasized that the ferromagnetism is *not saturated* as in the case of these models. In the case of the ferromagnetic Kondo model, the phase–separated state was found near half-filling. However, it was pointed out that such a phase–separated state can arise at low densities if an antiferromagnetic Heisenberg coupling is added to the model. Several studies in different numbers of dimensions using different methods suggest that the phase–separated state is very robust. It is also mentioned that the inclusion of longer–range Coulomb repulsion can turn the phase–separated state into more exotic phases, such as striped phases with ferromagnetic domains. While we have only studied a one-dimensional system, the arguments presented for the physical mechanism of phase separation should still be valid in higher dimensionsal systems.

Also, it is important to notice that the Anderson model can be mapped to the antiferromagnetic Kondo model for large values of the Coulomb repulsion. It is well known that a ferromagnetic phase is also present in the antiferromagnetic Kondo lattice model.[13] However, there is no phase–separated state because the antiferromagnetic coupling is higher order than the mapping. We believe that an additional antiferromagnetic Heisenberg coupling of appropriate strength between the localized spins would induce a phase–separated state in the Kondo lattice model.

In the second part of our work, we have studied the d–p model the parameters to values relevant to the cuprates. We have found that the sign of the oxygen hopping t_{pp} is crucial in determining the physics of the ground state. Three disconnected ferromagnetic phases were found in the phase diagram. One phase occurs at positive t_{pp} and is similar to the ferromagnetic phase found in the PAM and discussed in the first part of this work. A second phase appears for negative t_{pp} at and near quarter filling and occurs at a point at which the occupied noninteracting band has a flat dispersion. This "flat-band" mechanism is in agreement with a picture based on exact theorems.[6,7] A third ferromagnetic phase appears for small negative t_{pp} and it is related to ferromagnetic electron exchange processes on plaquettes with a positive product of hopping integrals. This phase has elements of ferrimagnetism due to an ordering of triangular plaquettes with a ferromagnetic moment and isolated, antiferromagnetically aligned d–holes.

ACKNOWLEDGMENTS

We thank S. Trugman and S. Daul for helpful discussions. M. Guerrero acknowledges the support of the U. S. Department of Energy. R.M.N acknowledges an allocation of computer time from the Centro Svizzero di Calcolo Scientifico in Manno and support from the Swiss National Foundation under Grant Nos. 20–46918.96 and 20–53800.98.

[1] M.C. Gutzwiller, Phys. Rev. Lett. **10**, 159 (1963); J. Hubbard, Proc. Roy. Soc. **A276**, 238 (1963); J. Kanamori, Prog. Theor. Phys. **30**, 275 (1963).
[2] P. Fazekas, Phil. Mag. B **76**, 797 (1997).
[3] D. Vollhardt *et al.*, Z. Phys. B **103**, 283 (1997); D. Vollhardt *et al.*, cond-mat/9804112 (to appear in *Advances in Solid State Physics*, Vol. 38).
[4] S. Daul and R.M. Noack, Phys. Rev. B **58**, 2635 (1998).
[5] R. Hlubina, S. Sorella and F. Guinea, Phys. Rev. Lett. **78**, 1343 (1997).
[6] A. Mielke, Phys. Lett. A **174**, 443 (1993).
[7] A. Mielke and H. Tasaki, Commun. Math. Phys. **158**, 31 (1993).
[8] R. Strack and D. Vollhardt, Phys. Rev. Lett. **72**, 3425 (1994).
[9] E. Lieb and D. Mattis, Phys. Rev. **125**,164 (1962).
[10] H. Tasaki, unpublished, cond-mat/9512169.
[11] K. Penc, H. Shiba, F. Mila and T. Tsukagoshi, Phys. Rev. B **54**, 4056 (1996).
[12] M. Guerrero and R.M. Noack, Phys. Rev. B **53**, 3707 (1996).
[13] H. Tsunetsugu, M. Sigrist, and K. Ueda, Rev. Mod. Phys. **69**, 809 (1997).
[14] C.M. Varma, S. Schmitt-Rink and E. Abrahams, Solid State Commun. **62**, 681 (1987).
[15] K. Sano and Y. Ōno, J. Phys. Soc. Jpn. **67**, 389 (1998).
[16] A. Sudbø, C.M. Varma, T. Giamarchi, E.B. Stechel and R.T. Scalettar, Phys. Rev. Lett. **70**, 978 (1993).
[17] K. Sano and Y. Ōno, Physica C **205**, 170 (1993); K. Sano and Y. Ōno, Physica C **242**, 113 (1995).
[18] M. Grilli, R. Raimondi, C. Castellani and C. Di Castro, Phys. Rev. Lett. **67**, 259 (1991).
[19] Y. Nagaoka, Phys. Rev. **147**, 392 (1966).
[20] S. R. White, Phys. Rev. Lett. **69**, 2863 (1992); Phys. Rev. B **48**, 10345 (1993).
[21] I. Peschel, X. Wang, M. Kaulke and K. Hallberg, eds., *Density Matrix Renormalization: A New Numerical Method in Physics*, Springer Verlag, Berlin, 1999.
[22] B. Möller and P. Wölfle, Phys. Rev. B **48**, 10320 (1993).
[23] F.C. Zhang and T.M. Rice, Phys. Rev. B **37**, 3759 (1988).
[24] M. Sigrist, H. Tsunetsugu, K. Ueda and T.M. Rice, Phys. Rev. B **46**, 13838 (1992).
[25] T. Yanagisawa and Y. Shimoi, Phys. Rev. B **48**, 6104 (1993).
[26] H. Bethe, Z. Physik **71**, 205 (1931).
[27] R.L. Martin, Phys. Rev. B **53**, 15501 (1996).
[28] A. Moreo, S. Yunoki and E. Dagotto, Science **283**, 5410 (1999).